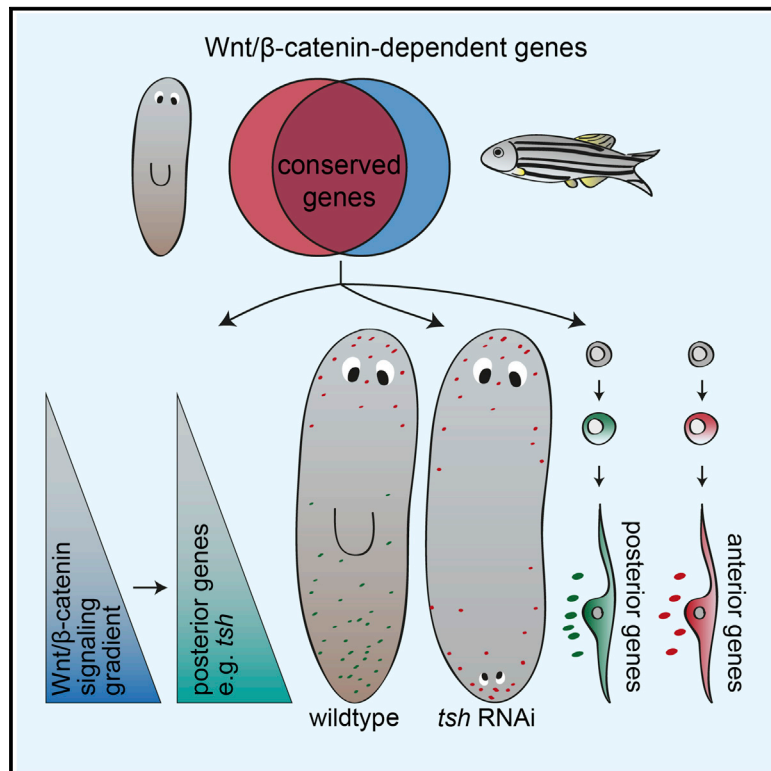


β -Catenin-Dependent Control of Positional Information along the AP Body Axis in Planarians Involves a Teashirt Family Member

Graphical Abstract



Authors

Hanna Reuter, Martin März, ...,
Gilbert Weidinger, Kerstin Bartscherer

Correspondence

kerstin.bartscherer@mpi-muenster.mpg.de

In Brief

Reuter et al. used transcriptome analyses to identify conserved downstream targets of Wnt/β-catenin signaling and their cellular sources in planarians. They discovered *teashirt* as a regulator of regeneration polarity and provide insights into β-catenin-mediated control of positional information along the planarian anterior-posterior body axis.

Highlights

- Regeneration involves conserved β-catenin-dependent genes in planarians and fish
- A β-catenin-dependent *teashirt* gene controls tissue polarity in planarians
- β-catenin RNAi induces the differentiation of muscle cells with anterior identity

Accession Numbers

KP003814
KP003815
KP003816
KP003817
KP003818



β -Catenin-Dependent Control of Positional Information along the AP Body Axis in Planarians Involves a Teashirt Family Member

Hanna Reuter,^{1,2,3} Martin März,^{1,2} Matthias C. Vogg,^{1,2} David Eccles,⁴ Laura Grifol-Boldú,^{1,5} Daniel Wehner,⁶ Suthira Owlarn,^{1,2,3} Teresa Adell,⁵ Gilbert Weidinger,⁶ and Kerstin Bartscherer^{1,2,*}

¹Max Planck Research Group for Stem Cells and Regeneration, Max Planck Institute for Molecular Biomedicine, Von-Esmarch-Strasse 54, 48149 Münster, Germany

²Medical Faculty, University of Münster, Albert-Schweitzer-Campus 1, 48149 Münster, Germany

³CiM-IMPRS Graduate School, Schlossplatz 5, 48149 Münster, Germany

⁴Malaghan Institute of Medical Research, Victoria University, Kelburn Parade, Wellington 6242, New Zealand

⁵Department of Genetics and Institute of Biomedicine, University of Barcelona, 08028 Barcelona, Catalonia, Spain

⁶Institute for Biochemistry and Molecular Biology, Ulm University, Albert-Einstein-Allee 11, 89081 Ulm, Germany

*Correspondence: kerstin.bartscherer@mpi-muenster.mpg.de

<http://dx.doi.org/10.1016/j.celrep.2014.12.018>

This is an open access article under the CC BY-NC-ND license (<http://creativecommons.org/licenses/by-nc-nd/3.0/>).

SUMMARY

Wnt/ β -catenin signaling regulates tissue homeostasis and regeneration in metazoans. In planarians—flatworms with high regenerative potential—Wnt ligands are thought to control tissue polarity by shaping a β -catenin activity gradient along the anterior-posterior axis, yet the downstream mechanisms are poorly understood. We performed an RNA sequencing (RNA-seq)-based screen and identified hundreds of β -catenin-dependent transcripts, of which several were expressed in muscle tissue and stem cells in a graded fashion. In particular, a *teashirt* (*tsh*) ortholog was induced in a β -catenin-dependent manner during regeneration in planarians and zebrafish, and RNAi resulted in two-headed planarians. Strikingly, intact planarians depleted of *tsh* induced anterior markers and slowly transformed their tail into a head, reminiscent of β -catenin RNAi phenotypes. Given that β -catenin RNAi enhanced the formation of muscle cells expressing anterior determinants in tail regions, our study suggests that this pathway controls tissue polarity through regulating the identity of differentiating cells during homeostasis and regeneration.

INTRODUCTION

Planarians are flatworms with high regenerative potential, which use pluripotent stem cells as the cellular source for new tissues (Wagner et al., 2011). Upon tissue amputation, planarians initiate a regenerative response that involves enhanced proliferation and differentiation of stem cells, resulting in the formation of a regeneration blastema (Wenemoser and Reddien, 2010). In intact animals, stem cells are thought to continuously replace dying cells

from differentiated tissues (Pellettieri et al., 2010). How they are informed about their relative position within the tissue and instructed to generate anterior or posterior cell types is largely unknown.

Wnts are conserved signaling molecules that, in many contexts, induce transcriptional changes in target cells through the stabilization of β -catenin and subsequent activation of β -catenin-dependent genes (Clevers, 2006). In contrast to other organisms, where β -catenin is a bifunctional protein controlling both Wnt-mediated signaling and cell-cell adhesion, β -catenin in the planarian species *Schmidtea mediterranea* displays a structural and functional segregation into SMED- β -CATENIN-1 and SMED- β -CATENIN-2, of which SMED- β -CATENIN-1 exclusively functions in the Wnt signaling pathway (Chai et al., 2010). Strikingly, RNAi-mediated silencing of *Smed- β -catenin-1* as well as *Smed-wnt1* and *Smed- β -catenin-1* (*evi/wls*) for simplicity) result in planarians that regenerate a head instead of a tail (Adell et al., 2009; Gurley et al., 2008; Iglesias et al., 2008; Petersen and Reddien, 2008, 2009), and β -catenin inhibition even induces head regeneration in regeneration-deficient species (Liu et al., 2013; Sikes and Newmark, 2013; Umesono et al., 2013). Conversely, RNAi against Wnt/ β -catenin antagonists, such as *APC* and *notum*, can cause the formation of ectopic tails at anterior wounds (Gurley et al., 2010; Petersen and Reddien, 2011), suggesting that Wnt/ β -catenin signaling suppresses head identity. Interestingly, otherwise intact planarians transform their tails into heads after β -catenin RNAi during tissue turnover (Gurley et al., 2008; Iglesias et al., 2008), indicating that this signaling pathway is not only important for regeneration polarity, but also for the maintenance of a polarized anterior-posterior (AP) axis.

Regulators of Wnt signaling are expressed in distinct regions along the AP axis of planarians (Gurley et al., 2010; Petersen and Reddien, 2009). Generally, Wnt signaling agonists, such as *wnt1*, *wnt11-1*, *wnt11-2*, *wnt11-5*, and *frizzled-4* (*fz-4*), are expressed mainly in posterior regions (Adell et al., 2009; Gurley et al., 2010; Petersen and Reddien, 2009), whereas antagonists, such as *secreted frizzled receptor-like-1* (*sfrp-1*) and *notum*, are

concentrated in the anterior (Gurley et al., 2008, 2010; Petersen and Reddien, 2008, 2011). Both expression patterns and RNAi phenotypes suggest that a Wnt activity gradient might control AP polarity, with high activity in the tail and low activity in the head (Adell et al., 2010).

Recently, it was proposed that subepidermal muscle cells are the cellular source of positional information by expressing position control genes (PCGs) such as genes encoding WNTs and their inhibitors (Witchley et al., 2013). After tissue loss, muscle cells adjacent to the site of injury change their PCG expression profile, possibly as an interpretation of their new relative position along the body axes. They might therefore generate a flexible and dynamic coordinate system for positional information in planarians. How this coordinate system is established during regeneration and maintained during tissue turnover has not been addressed.

Here, we show that β -catenin is required for the graded expression of genes along the AP axis in muscle cells and stem cells and that β -catenin RNAi leads to the formation of posterior muscle cells that express anterior PCGs. An RNA sequencing (RNA-seq)-based screen resulted in the discovery of a *teashirt* (*tsh*) ortholog, whose expression is induced during planarian and vertebrate regeneration in a β -catenin-dependent manner. *tsh* RNAi in planarians revealed striking similarities to the β -catenin RNAi phenotypes. We propose a model in which Wnt/ β -catenin signaling controls tissue polarity through regulating the identity of newly forming cells expressing positional determinants.

RESULTS

An RNA-Seq-Based Screen Reveals β -Catenin-Dependent Genes in Planarians

To identify regulators of β -catenin-mediated polarity decisions in planarians, we set out to analyze the transcriptome of β -catenin RNAi planarians. Because this treatment causes an anteriorization of planarians (Gurley et al., 2008; Iglesias et al., 2008; Petersen and Reddien, 2008), we chose a time point after double-stranded RNA (dsRNA) injection at which the β -catenin knockdown was efficient but ectopic anterior tissues, such as the brain and eyes, were not yet visible (Figures 1B, S1A and S1B). We used tail fragments of β -catenin and control (*gfp*) RNAi animals 7 days after the last dsRNA injection (dpin) (day 16 after the first dsRNA injection) for deep sequencing (RNA sequencing [RNA-seq]) (Figure 1A). By comparing the transcriptomes of β -catenin and control RNAi planarians, we identified 440 downregulated transcripts upon β -catenin RNAi ($p < 0.05$, fold change < 0.5) and 348 upregulated transcripts ($p < 0.05$, fold change > 2) (Figure 1B; Data S1). Among the genes with reduced transcript expression were posterior-enriched genes, such as the homeobox transcription factor genes *abdBa* and *hoxD* (Iglesias et al., 2008; Nogi and Watanabe, 2001; Orii et al., 1999), *wnt11-1* and *wnt11-2* (Petersen and Reddien, 2009), *axinB* (Iglesias et al., 2011), *fz-4* (Gurley et al., 2008), *evl/wls* (Adell et al., 2009), and *prep* (Felix and Aboobaker, 2010). Induced genes after β -catenin RNAi included the anterior genes *sfrp-1* (Petersen and Reddien, 2008) and *nou-darake* (*ndk*) (Cebrià et al., 2002; Figures 1B and 1C; Data S1).

Because the loss of β -catenin causes the transformation of tails into heads in homeostatic planarians (Gurley et al., 2008; Iglesias et al., 2008; Petersen and Reddien, 2008), we compared our data set to previously published gene expression data from head and tail fragments (Kao et al., 2013). We found that 63% of the upregulated transcripts in the β -catenin RNAi data set were enriched in the head and 14% of the downregulated transcripts were enriched in the tail of wild-type planarians, suggesting that part of the data set reflects the loss of posterior and gain of anterior identity (Figure S1C; Data S2).

β -Catenin-Dependent Genes Are Expressed in Distinct Patterns along the AP Axis

We next chose 70 genes with the highest and most significant reduction in expression levels after β -catenin RNAi (Figure 1B; Data S1) to determine their expression domains in a whole-mount in situ hybridization (WISH) screen. Interestingly, 35% of the transcripts analyzed displayed differential expression along the AP axis (25/70) with high expression in the tail (Data S1). Among those were members of the *sp*- and *teashirt* (*tsh*) families of transcription factor genes (*Smed-sp5: tr5_10125*, *Smed-tsh: tr5_11049*), a putative *ptk7* (*smed-ptk7: tr5_7361*) and a α 1-macroglobulin (*tr5_6831*) ortholog, and a gene with no obvious homology (*tr5_12233*) (Figure 1D; Table S1; Data S1). Nine of these 25 sequences revealed expression in or around the pharynx, and several were also expressed in the nervous system. Among the remaining 45/70 β -catenin-dependent sequences, 21 were expressed in cells within or in proximity to the digestive system (Figures 1E and 2A–2C; Table S1; Data S1). Nine of those localized to distinct cells along the gut, including sequences similar to peptidases (*tr5_785*, *tr5_4416*, *tr5_3835*). Others were more broadly expressed (e.g., *tr5_6444* and *tr5_2051*). Furthermore, three of 70 transcripts (*tr5_905*, *tr5_1052*, *tr5_6704*) showed peripheral expression in distinct cells evenly distributed along the AP axis (Figure S1D), one of them (*tr5_905*) being known as an early stem cell progeny marker (*NB.32.1g*) (Eisenhoffer et al., 2008). Seven of 70 transcripts showed expression patterns distinct from the previous categories, and for 14 no conclusive expression patterns were obtained (Data S1).

We validated β -catenin dependency and analyzed 40/70 candidate genes, including genes from all expression categories, in homeostatic β -catenin RNAi animals at 7 dpin. The graded expression of 18/22 genes along the AP axis was strongly inhibited upon β -catenin depletion, and at least some of them were induced after *APC* RNAi (Figure 1D; Data S1). Accordingly, nine of nine examined gut-associated sequences were strongly reduced upon β -catenin RNAi, confirming the RNA-seq results (Figure 1E; Data S1).

We further analyzed 20 transcripts, whose expression was strongly induced after β -catenin RNAi (Figures 1B and 1F; Data S1; Table S1). These transcripts were mainly expressed in the anterior body parts in control animals, ranging from a broad expression within the head to specific expression in the brain or in cells in the head periphery. Strikingly, these sequences were strongly induced at the tip of the tail and sometimes in lateral regions after β -catenin RNAi at 7 dpin (Figure 1F). In addition, those expressed in the brain of control RNAi animals (*tr_23878*, *tr_10443*) extended toward the posterior after

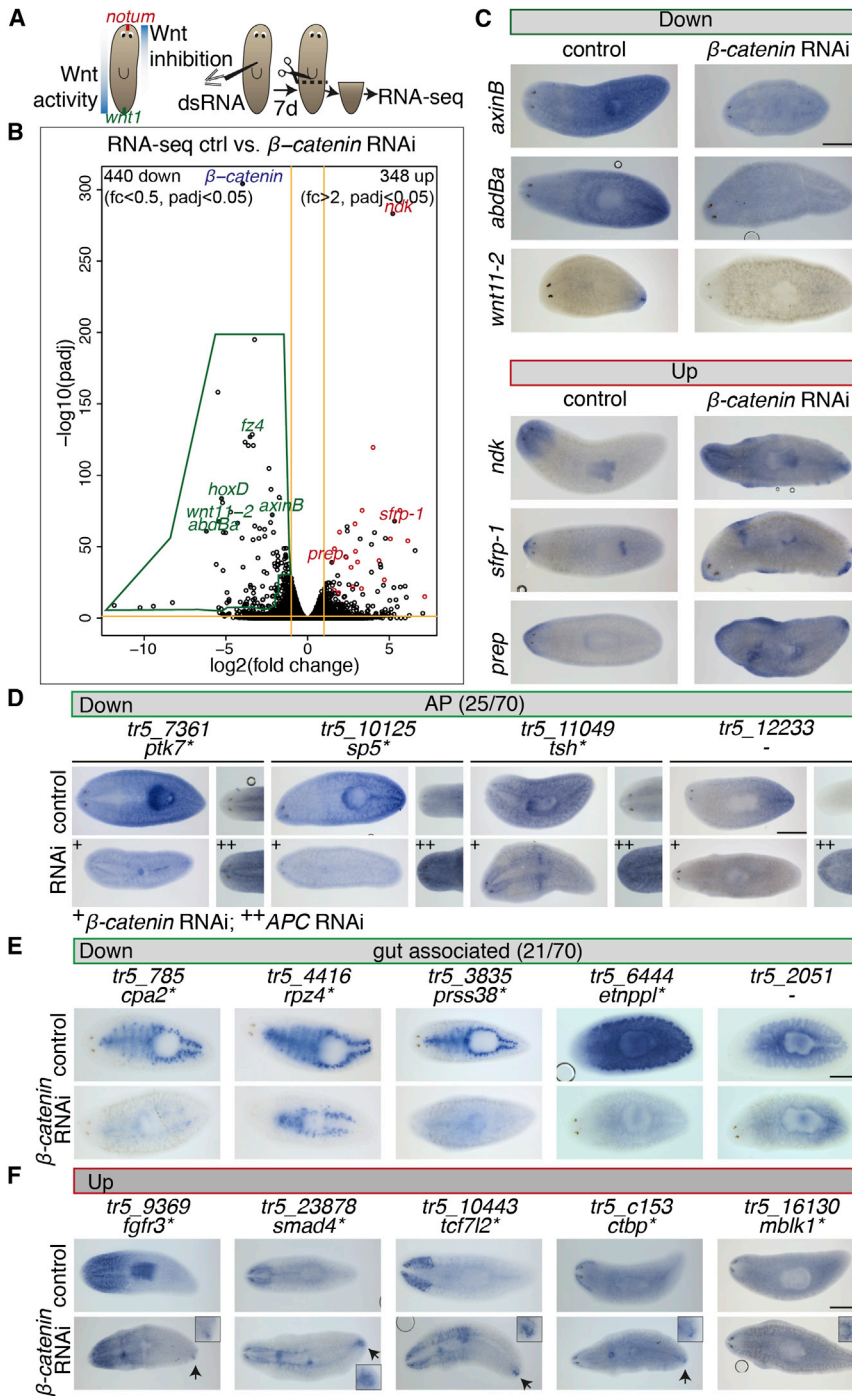


Figure 1. An RNA-Seq Approach Reveals β -Catenin-Dependent Genes

(A) Experimental set-up. (B) Volcano plot illustrating \log_2 of fold change expression versus $-\log_{10}$ of adjusted p value (padj). Only genes with baseMean > 0 in both samples are plotted. Thresholds are indicated in yellow: adjusted p value: < 0.05 ; \log_2 (fold change) > 1 (upregulated after β -catenin RNAi compared to control RNAi; 348 transcripts) and < -1 (downregulated after β -catenin RNAi compared to control RNAi; 440 transcripts). Candidate genes chosen for further analysis are within the green frame. Red circles mark selected upregulated genes. (C–F) (C) WISH of indicated transcripts on control (wild-type), β -catenin, or APC RNAi planarians. (D) 25/70 genes revealed a graded expression along the anterior-posterior (“AP”) axis. Four representative transcripts are shown, displaying a strong reduction after β -catenin RNAi 7 days after last injection (dpin), and an induction in the anterior region after APC RNAi 21 dpin. (E) 21/70 genes were expressed along the digestive system (“gut associated”). Five representative transcripts are shown at 7 dpin. (F) Five upregulated genes with induced expression in the tail of β -catenin RNAi animals at 7 dpin are shown (arrows and insets). Scale bar, 500 μ m in (C)–(F). Transcripts marked with asterisk are annotated based on their top BLASTx hit. See also Figure S1, Table S1, and Data S1.

different categories with fluorescent in situ hybridization (FISH) using cell-type-specific markers. This allowed us to localize the expression of nine candidates to relatively large cells along the gut (Figures 1E and 2A). Interestingly, an antibody against one candidate, SMED-RAPUNZEL-1 (RPZ-1; *tr5_4416*), recognized proteins in large granules in these cells (Figure 2B), suggesting that they might be secretory goblet cells (Zayas et al., 2010). Other candidate genes, such as *tr5_1296*, were broadly coexpressed with a gut marker (Figure 2C), and those candidate-expressing cells were surrounded by a collagen-positive cell layer, presumably muscle cells (Figure S2A).

The second major group of candidate transcripts showed graded expression patterns along the AP axis. FISH using

β -catenin depletion, confirming a posterior-to-anterior transformation of these animals.

Graded Expression of β -Catenin-Dependent Genes along the AP Axis Occurs in Subepidermal Muscle Cells and in Stem Cells

To test which cells respond to β -catenin signaling in planarians, we further analyzed the expression of several transcripts from

pooled probes against several of them revealed a decreasing fluorescent intensity from posterior to anterior (Figure 2D), strengthening the hypothesis that a β -CATENIN activity gradient may control gene expression, with highest activity in the tail. It was previously shown that collagen-positive muscle cells in subepidermal regions are the cellular source of positional information by expressing position control genes (PCGs). Among the PCGs expressed in muscle cells are *fz-4*, *sfrp-1*, *wnt11-1*, *-2*,

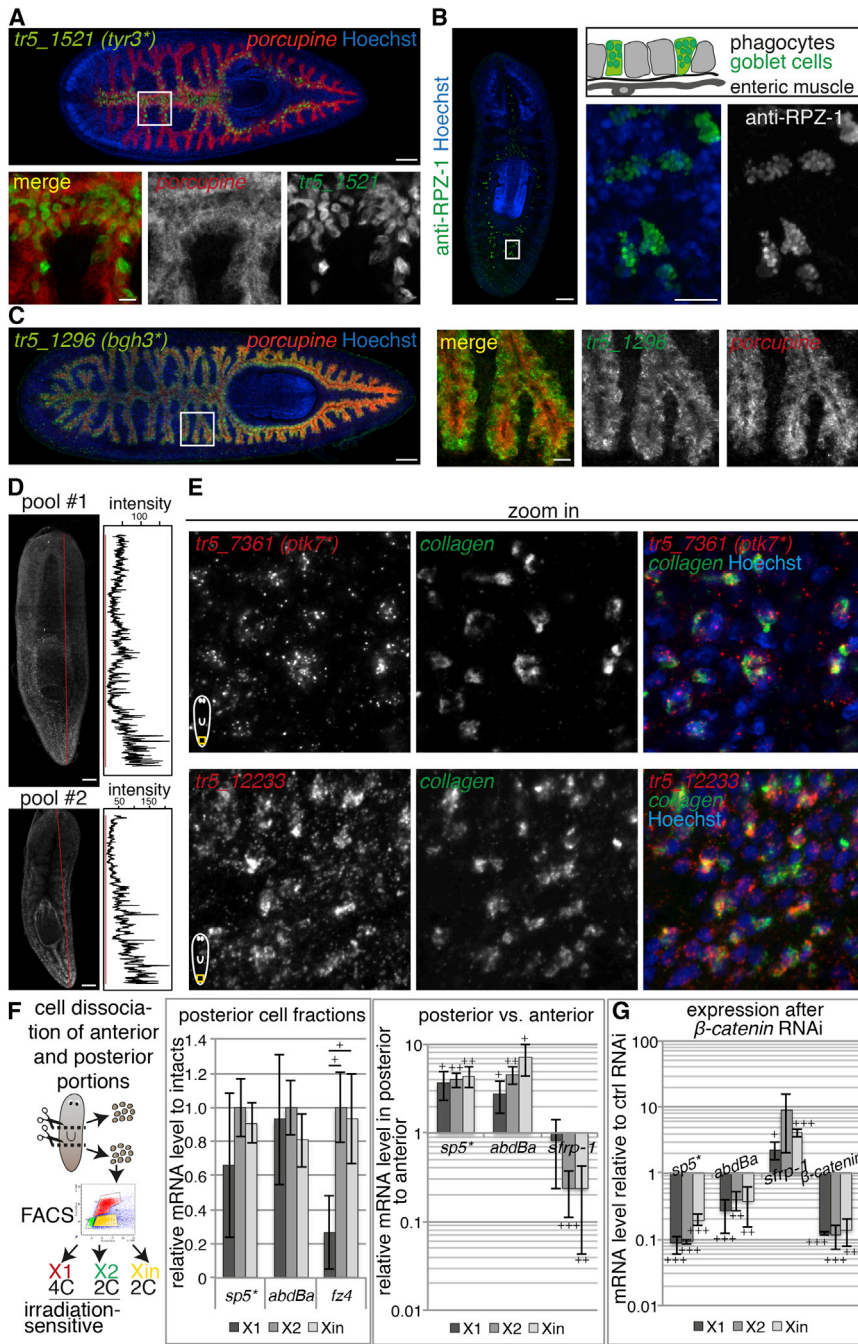


Figure 2. β -Catenin-Dependent Genes Are Expressed in Various Cell Types

(A) Double FISH of *tr5_1521* (green) with the gut marker *porcupine* (red) reveals expression in distinct cells along the main and primary branches of the gut in intact animals.

(B) Anti-RPZ-1 immunostaining (green) in intact animals reveals its localization to large granules. The scheme depicts the localization of putative goblet cells within the planarian gut epithelium.

(C) Double FISH of *tr5_1296* (green) and the gut marker *porcupine* (red) in intact animals.

(D) FISH on intact animals using pooled probes (#1: *tr5_7361*, *tr5_12233* and *wnt11-5*; #2: *tr5_10125*, *tr5_11049*, *abdBa*). Signal intensities measured along AP (red line) are displayed in the neighboring plot.

(E) High-magnification pictures show cells expressing candidate genes *tr5_7361* or *tr5_12233* (red) and the muscle marker gene *collagen* (green) in the subepidermal region.

(F and G) qPCR analysis on cell fraction X1 (4C), X2 (2C), and Xin (2C; irradiation insensitive) isolated by FACS according to size and DNA content. (F) Left panel displays expression of *sp5**, *abdBa*, and *fz4* in cell fractions isolated from post-pharyngeal tissue. Expression levels were normalized to intact and percentage of peak expression is shown. The right panel shows the expression of *sp5**, *abdBa*, and *sfrp-1* in post-pharyngeal (posterior) versus prepharyngeal (anterior) cell fractions. Expression levels of posterior cell fractions were normalized to their respective anterior cell fractions. (G) Differential expression of *sp5**, *abdBa*, and *sfrp-1* in all cell fractions after β -catenin RNAi is shown. Expression levels of cell fractions isolated from homeostatic β -catenin RNAi animals 7 days after last injection were normalized to their respective control RNAi cell fractions.

Error bars represent SDs of three biological replicates. Significances (Student's t test) are indicated (+, $p \leq 0.05$); (++, $p \leq 0.01$); (+++, $p \leq 0.001$). Transcripts marked with asterisk are annotated based on their top BLASTx hit. Scale bars, 100 μ m in (A)–(E) (overview), 20 μ m in (A)–(D) (zoom). DNA is blue (Hoechst). Boxes mark the zoom-in region. See also Figure S2.

-5, and *evi/wls* (Witchley et al., 2013), genes whose expression levels were strongly reduced after β -catenin RNAi. We tested some other candidates for their localization in subepidermal muscle cells. Using *collagen* as a marker (Witchley et al., 2013), FISH detection of *tr5_12233* and *ptk7* mRNAs revealed that this is indeed the case (Figures 2D and 2E). Notably, some of the *collagen*-positive cells that also differentially expressed such candidate transcripts along the AP axis were located close to the gut epithelium (Figures S2A–S2C), suggesting that in

addition to subepidermal muscle cells, intestinal muscle cells might express β -catenin-dependent PCGs.

Interestingly, the candidate genes *sp5* and *abdBa* were recently found to be expressed in subpopulations of stem cells (van Wolfswinkel et al., 2014). To investigate whether stem cells differentially express candidate genes along the AP axis, we isolated three different cell populations by fluorescence-activated cell sorting (FACS) according to their size and DNA content (Hayashi et al., 2006) from anterior and posterior fragments and

analyzed gene expression by quantitative PCR (qPCR). *sp5* and *abdBa* transcripts were found in all three cell fractions derived from tail tissue: an irradiation-sensitive fraction with high DNA content (>2C) enriched in stem cells in S/G2/M phases of the cell cycle (X1); a partially irradiation-sensitive fraction with 2C DNA content containing stem cells in G1 and small progeny (X2); and an irradiation-insensitive fraction composed of differentiated cells (Xin) (Figure 2F). In contrast, the known PCG *fz-4* was mainly expressed in posterior X2 and Xin cell fractions (Figure 2F). Strikingly, the levels of *sp5* and *abdBa* transcripts were higher in all cell fractions derived from tail tissue compared to the anterior fractions (Figure 2F), and their expression was strongly reduced in all cell fractions after β -catenin RNAi (Figure 2G). Consistent with this, *sfrp-1* expression, an anterior PCG, was higher in anterior cell fractions and was induced after β -catenin RNAi (Figures 2F and 2G). These data suggest that stem cells respond to differential β -catenin signaling along the AP axis.

Interestingly, we found two β -catenin-dependent genes (*tr5_1052* and *tr5_6704*), which were coexpressed with the early progeny marker *NB.32.1g* (Eisenhoffer et al., 2008) in the same cells (Figure S2D; Table S1; Data S1). Because *NB.32.1g* marks an epithelial cell lineage giving rise to the epidermis (van Wolfswinkel et al., 2014), this lineage may respond to changes in β -CATENIN levels.

Comparisons to β -Catenin Gain-of-Function and to Zebrafish Regeneration Transcriptomes Reveal High-Confidence and Conserved Wnt/ β -Catenin-Dependent Genes

During planarian regeneration, the secreted Wnt inhibitor NOTUM is thought to regulate early polarity decisions through inhibition of wound-induced WNTs at anterior-facing wounds (Petersen and Reddien, 2011). Thus, we reasoned that inhibition of *notum* expression might induce β -catenin-dependent genes and analyzed the transcriptome of tail stumps of *notum* and control RNAi animals at 18 hr after amputation (hpa) (Figure 3A) (Data S3), a time when anterior *notum* expression is prominent. We found 38 of the downregulated genes in the β -catenin RNAi data set as induced after *notum* RNAi. Among those genes were *hoxD*, *wnt11-1*, and *wnt11-2*, *fz-4*, *abdBa*, *sp5*, and *tsh*. Conversely, 16 of the upregulated sequences were reduced after *notum* RNAi, including *ndk* and *sfrp-1*. Because these 54 transcripts were differentially expressed after *notum* RNAi during the first few hours in the regeneration process, they might represent Wnt-dependent genes involved in polarity decisions in planarians (“Wnt/ β -catenin-dependent gene set”). Interestingly, whereas ten of 25 β -catenin-dependent genes in the AP category were upregulated after *notum* RNAi, none of the gut-associated genes was affected (Figure S3A). This is consistent with expression analysis of candidate genes after *APC* RNAi, where *sp5* and *tsh* were highly induced, yet gut-associated genes, such as *rpz-1*, were not (Figure 1D; Figure S3B). Together these data suggest that some β -catenin-dependent genes of the AP category respond directly to alterations in Wnt/ β -catenin signaling, whereas gut-associated genes might be affected indirectly through gut remodeling processes induced after polarity changes.

Although whole-body regeneration is only found in invertebrates, some vertebrates, including zebrafish, do display a high regenerative potential. They can robustly regenerate several organs, including the heart, the brain, and their fins. Wnt/ β -catenin signaling is essential for fin regeneration (Kawakami et al., 2006; Stoick-Cooper et al., 2007). Recently, we analyzed the Wnt/ β -catenin targetome in the regenerating caudal fin utilizing *hsp70l:dkk1-GFP^{w32}* (*hs:dkk1*; (Stoick-Cooper et al., 2007) and *hsp70l:Mmu.Axin1-YFP^{w35}* (*hs:Axin1*; Kagermeier-Schenk et al., 2011) transgenic fish lines, which allow for heat shock-inducible overexpression of the Wnt/ β -catenin signaling antagonists *dkk1* and *axin1* (Wehner et al., 2014). We set out to compare the planarian and zebrafish Wnt/ β -catenin targetomes and blasted the 54 sequences of the planarian Wnt/ β -catenin-dependent gene set against the zebrafish RefSeq database. Thirty-three of 54 sequences resulted in a BLAST hit, and 23 of those showed similar expression regulations as functionally similarly grouped zebrafish genes in at least one of the zebrafish data sets (Table 1). Among the overlapping Wnt/ β -catenin-dependent genes of both animals were genes encoding Frizzleds, Wnts, and Homeobox transcription factors. Interestingly, six of ten candidate genes differentially expressed along the AP axis in planarians and undergoing β -catenin as well as *notum*-dependent regulation in planarians (Figures 1D, 3A, and S3A) were similarly regulated in zebrafish (Figure S3C).

Taken together, the overlap of similarly regulated genes in regenerating fish and planarians suggests that the general requirement for Wnt/ β -catenin signaling in highly regenerative organisms is reflected by a shared set of target genes.

Expression of *teashirt* is β -Catenin-Dependent in Regenerating Planarians and Zebrafish Fins

Two genes present in planarian and zebrafish data sets, *tsh* and zebrafish *tshz2*, encode members of the Tsh-related zinc finger protein family according to phylogenetic analysis (Tables 1 and S2; Figures S3D and S3E). Although *tsh* genes have been suggested to act as homeotic genes and Wnt signaling modulators during *Drosophila* and *Xenopus* development (Fasano et al., 1991; Gallet et al., 1998; Koebernick et al., 2006), they have not been linked to Wnt/ β -catenin signaling and regeneration in planarians or fish.

In planarians, *tsh* was induced at anterior and posterior regeneration sites from 18 hpa onward (Figure 3B; Figures S3F and S3G). At the anterior amputation site, *tsh* expression was found in the regenerating brain after 3 days postamputation (dpa) (Figures 3B and 3C). *tsh* levels were strongly reduced after β -catenin RNAi and ectopically induced after *APC* RNAi at anterior regeneration sites (Figure 3C). Accordingly, *tsh* expression was inhibited by RNAi against different combinations of *wnt* genes (Figure 3D). Similarly, in zebrafish, *tshz2* was robustly detected in caudal as well as pectoral fin regenerates 3 days following amputation. This expression was strongly reduced 6 hr after heat shock-mediated induction of the Wnt/ β -catenin signaling inhibitors *dkk* or *axin1* (Figure 3E). Hence, *tsh* genes are induced in regenerating tissues in planarians and fish in a Wnt/ β -catenin-dependent manner.

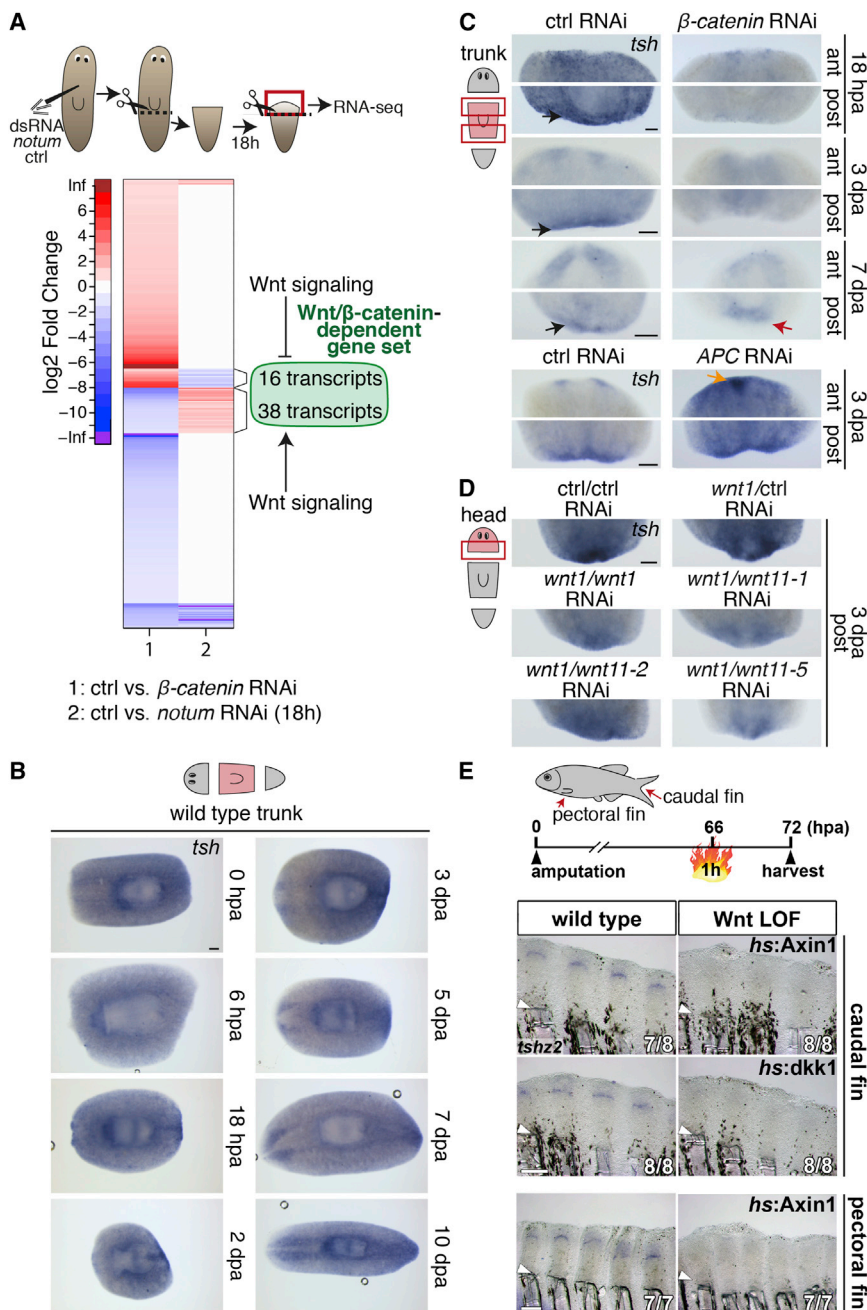


Figure 3. *tsh* Genes Are Induced in Regenerating Tissues of Planarians and Zebrafish in a Wnt/ β -Catenin-Dependent Manner

(A) Experimental set-up for the identification of differentially expressed (DE) genes after *notum* RNAi, 18 hr postamputation (hpa). Heatmap of DE genes (n = 367) after β -catenin and *notum* RNAi according to their log₂ fold change (control versus *notum* or β -catenin RNAi) (adjusted p value <0.05). Upregulation is indicated in red; downregulation is in blue. Note that 16 upregulated and 38 downregulated transcripts after β -catenin RNAi are inversely regulated after *notum* RNAi.

(B) WISH time course of *tsh* expression during regeneration of planarian trunk fragments.

(C) *tsh* expression at anterior and posterior regeneration sites of ctrl (control) trunk fragments and after β -catenin or *APC* RNAi at indicated regeneration time points. Black arrow; posterior *tsh* expression; red arrow: ectopic posterior brain; orange arrow: ectopic anterior *tsh* expression.

(D) Posterior *tsh* expression in control RNAi head fragments 3 dpa is reduced after *wnt1* RNAi. Note that simultaneous knockdown of *wnt11-1/-2* and *-5* enhances the effect of *wnt1* RNAi on *tsh* expression.

(E) Zebrafish *tshz2* is robustly expressed in caudal and pectoral fin regenerates at 72 hpa, and its expression is strongly reduced upon over-expression of the Wnt/ β -catenin antagonists *axin1* or *dkk1* for 6 hr in *hs:Axin1* or *hs:dkk1* transgenic fin regenerates. Arrowhead: amputation plane. Numbers indicate the number of fins showing the depicted expression pattern and the total number of fins analyzed.

Scale bar, 100 μ m in (B)–(D), 200 μ m in (E). See also Figure S3, Data S3, and Table 1.

RNAi against *teashirt* Generates Two-Headed Planarians

To test for a putative function of *tsh* in AP polarity, we depleted *tsh* by RNAi, amputated heads and tails, and allowed regeneration to take place. This resulted in severe tail regeneration defects, whereas head regeneration appeared unaffected (Figures 4A, 4B, S4A, and S4B). Strikingly, 70% of *tsh* RNAi trunk fragments regenerated a head instead of a tail. This head was characterized by a pair of eyes (Figures 4A and 4B), and an accumulation of neurons, which appeared organized into a brain-like structure (Figures 4B and S4A). Occasionally, *tsh*

also during homeostasis and becomes visible within 3 weeks (Figure S1A). Hence, we analyzed *tsh* loss of function phenotypes during normal tissue turnover. Interestingly, ectopic posterior heads were visible in eight of ten animals, 3 months after the first dsRNA injection (Figures 4C and 4D). This obvious delay in phenotype was also represented by the presence of posterior Wnt transcripts at 12 dpi, a time when they were undetectable after β -catenin RNAi (Figure S4C) and is consistent with a delay of *tsh* RNAi-mediated polarity defects also in regenerating planarians (Figure S4D). These data suggest differences in either the strength or epistasis of *tsh* and β -catenin

Table 1. Wnt/ β -Catenin-Dependent Genes Identified in Both Planarians and Zebrafish

Group	<i>S. mediterranea</i> Transcript ID	<i>D. rerio</i> Gene Symbol
Downregulated upon Wnt Inhibition		
Wnts	<i>tr5_26416 (wnt11-2),</i> <i>tr5_17585 (wnt11-1)</i>	<i>wnt10a, wnt5b,</i> <i>wnt7aa, wnt9b</i>
Frizzled receptors	<i>tr5_13148 (fz4), tr5_17862</i>	<i>fzd10, fzd9b</i>
Homeobox transcription factors	<i>tr5_11570 (hoxD), tr5_23506, hoxa13a, hoxa5a</i> <i>tr5_17383 (abdBa)</i>	
Sp1-related transcription factors	<i>tr5_10125 (sp5)</i>	<i>sp5, sp8a, sp9,</i> <i>sp3, sp4</i>
Tsh family transcription factors	<i>tr5_11049 (tsh)</i>	<i>TSHZ2</i>
Matrix metalloproteinases	<i>tr5_3494</i>	<i>mmp11b</i>
Rapunzel proteins	<i>tr5_2682</i>	<i>rpz2, rpz5</i>
Cytochrome P450s	<i>tr5_7101</i>	<i>cyp24a1</i>
	<i>tr5_2542</i>	<i>stub1</i>
	<i>tr5_3563</i>	<i>podxl</i>
Upregulated upon Wnt Inhibition		
Secreted frizzled proteins	<i>tr5_10354 (sfrp-1)</i>	<i>sfrp2</i>
AP-2 transcription factors	<i>tr5_23253 (ap2)</i>	<i>tfap2a</i>
Eyes absent	<i>tr5_16977</i>	<i>eya2</i>
Fgf receptor(-like)	<i>tr5_9369, tr5_5721 (ndl-5),</i> <i>tr5_8594 (ndk), tr5_12428</i> <i>(ndl-4)</i>	<i>fgfr3</i>
Frizzled receptors	<i>tr5_10845</i>	<i>fzd8a</i>
Orthodenticle	<i>tr5_21187 (otxA)</i>	<i>otx2, otx5</i>

RNAi phenotypes, or in the downstream events that lead to their manifestation.

tsh Is Required for the Expression of wnt Genes at the Posterior Regeneration Pole and Restricts the Expression of Anterior Determinants

Tail regeneration is characterized by the wound-induced expression of *wnt1* in differentiated cells around the wound, the subsequent induction of posterior position control genes (PCGs), such as *wnt11-1*, *wnt11-2*, and *wnt11-5*, and the stem cell-dependent formation of a *wnt1*-positive cluster of cells at the posterior tip of the regeneration blastema by 3 dpa (Gurley et al., 2010; Petersen and Reddien, 2009). Interestingly, similar to a β -catenin loss of function scenario (Petersen and Reddien, 2009), *wnt1* induction at posterior wounds was normal after *tsh* RNAi at 18 hpa (Figure 4E), suggesting that *tsh* is required for regeneration polarity downstream of wound signaling and early *wnt1* expression. In contrast, stem cell-dependent expression of *wnt1* at the pole at 3 dpa, and that of *wnt11-1*, *wnt11-2*, and *wnt11-5*, was strongly inhibited (Figures 4E, S4E, and S4F).

The putative Wnt inhibitor *notum* is asymmetrically induced mainly at anterior-facing wounds (Petersen and Reddien, 2011) where it is thought to permit head specification. At later stages,

around 3 dpa, *notum* expression is found at the anterior regeneration pole, where it may contribute to proper head patterning, and in cells at the regenerating pharynx (Figure S4G). Interestingly, *notum*, like *sfrp-1*, was activated at posterior regeneration sites of *tsh* RNAi head fragments at 3 dpa (Figure 4F). We also tested for *notum* induction at posterior wounds of *tsh*-depleted head fragments at 18 hpa. Despite the ectopic formation of a posterior head, *notum* expression was not induced at posterior-facing wounds at 18 hpa (Figure 4G), suggesting that early *notum* expression is not necessary for head regeneration in the absence of *tsh*. Strikingly, in contrast to β -catenin RNAi regenerates, where *notum* is not detected at 18 hpa (Petersen and Reddien, 2011), *notum* expression was normal at anterior wound sites in *tsh* RNAi animals (Figure 4G).

tsh Is Coexpressed with Posterior Position Control Genes and Marks a Population of Stem Cells

Next, we tested if *tsh* and *wnts* are activated in the same cells. We performed double FISH experiments on intact planarians, where *wnt1* is expressed in a stripe of cells at the posterior midline, and on regenerating animals after 3 dpa. Interestingly, we found *tsh* transcripts in *wnt1*-positive cells in both scenarios (Figure 5A), and *wnt11-1*, *wnt11-2*, and *wnt11-5* expression coincided with *tsh* at 3 dpa (Figure S5A). In addition, *tsh* was expressed in a few cells in the anterior dorsal part of the head, at the pharynx, and in neurons of the brain and the ventral nerve cords of intact planarians (Figures 5B and S5B).

To our surprise, we also found *tsh*-expressing cells in the parenchyma, where stem cells reside, and this parenchymal expression was strongly reduced by 3 days after γ -irradiation (Figures 5B and S5B). Using the stem cell marker *smcdwi-1*, we confirmed expression of *tsh* in a subpopulation of stem cells by FISH (Figure 5C). Additionally, we found *tsh* transcripts in the stem cell-enriched X1/X2 fractions of FACS-sorted cells (Figure 5D). Particularly, *tsh* expression was higher in posterior than anterior cell fractions and was induced during regeneration at 3 dpa (Figure 5D). Consistent with the β -catenin-dependent expression of *sp5* and *abdBa* transcripts in stem cell-enriched FACS fractions (Figure 2F), *tsh* levels were strongly reduced in sorted cells from β -catenin RNAi animals (Figure 5D).

Tail-to-Head Transformation Is Irradiation Sensitive and Is Accompanied by Increased Cell Proliferation and Muscle Cell Production

Subepidermal collagen-positive cells, identified as muscle cells, are the cellular source for PCG expression (Witchley et al., 2013) and planarians induce anterior PCGs in posterior body regions after β -catenin (Gurley et al., 2008; Iglesias et al., 2008) (Figure 1C; Data S1) and *tsh* RNAi (Figures 4B and 4D). Two processes might be involved in the manifestation of this phenotype. First, existing muscle cells might alter their gene expression program through modified TSH/ β -CATENIN levels. Second, newly differentiating muscles may acquire anterior instead of posterior identity. We used β -catenin RNAi animals, which develop their phenotype within a few days after dsRNA injection, to test which scenario was more likely. *sfrp-1*-expressing cells ectopically accumulated at the posterior pole of homeostatic β -catenin

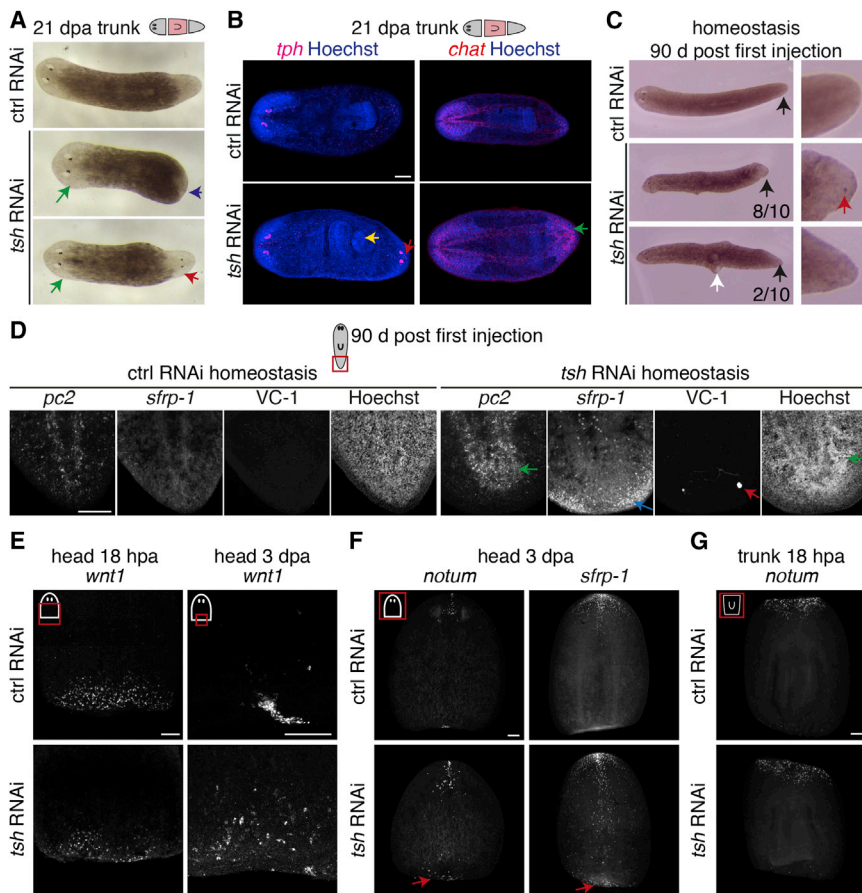


Figure 4. *tsh* RNAi Results in Two-Headed Planarians

(A) Regenerating trunk fragments of ctrl (control) and *tsh* RNAi animals 21 days postamputation (dpa). Blue arrows, impaired posterior regeneration; red arrows, ectopic posterior head; green arrows, normal anterior head regeneration. (B) Double FISH of *tph* (magenta) and *chat* (red) on regenerating trunk fragments (21 dpa) reveals posterior ectopic eye (red arrow) and brain (green arrow) formation in *tsh* RNAi animals. Yellow arrow, ectopic pharynx formation. DNA is blue. (C) Homeostatic *tsh* RNAi animals at 90 days after first dsRNA injection. *tsh* RNAi animals display lateral outgrowth (white arrow) and ectopic posterior eyes (black arrow) are shown. (D) Homeostatic ctrl or *tsh* RNAi animals at 90 days after first dsRNA injection. FISH of *pc2*, *sfrp-1*, VC-1-immunostaining, and Hoechst counterstaining reveal ectopic brain (green arrows) and eyes (red arrow) and the induction of the anterior marker *sfrp-1* (blue arrow) in *tsh* RNAi animals. (E) FISH for *wnt1* on ctrl or *tsh* RNAi head fragments at 18 hr postamputation (hpa) and 3 dpa. Note that wound-induced *wnt1* expression is not impaired at 18 hpa in *tsh* RNAi animals, whereas the cluster of posterior *wnt1* expression is lost at 3 dpa. Remaining *wnt1* expression in scattered cells is irradiation insensitive (see Figure S4F). (F) FISH on regenerating head fragments at 3 dpa reveals ectopic posterior *notum* and *sfrp-1* expression (red arrows) in *tsh* RNAi animals. (G) FISH for *notum* on ctrl or *tsh* RNAi trunk fragments at 18 hpa. *notum* is not ectopically induced at the posterior amputation site at this early time point. Scale bars, 100 μ m in (B) and (D)–(G). See also Figure S4.

RNAi animals and spread all along the edge of the animal (Figure 6A). Strikingly, expression of the muscle marker genes *collagen* and *myosin heavy chain (myhc)* as well as *myoD*, a marker for muscle progenitors in other systems (Buckingham and Rigby, 2014), was increased at the posterior pole and in some lateral regions (Figures 6B and S6A). *sfrp-1* and *collagen* expression in these regions coincided in most but not all cells (Figure 6C). Accordingly, mitotic cell numbers were significantly increased in the posterior (Figure 6D), raising the possibility that new muscle cells were formed. However, increased mitosis may be linked to remodeling processes as APC RNAi animals also displayed elevated mitotic activity at atypical sites (Figure S6B).

To test if ectopic *sfrp-1* expression requires stem cells, we depleted them by γ -irradiation before the first injection of dsRNA against β -catenin. Untreated β -catenin RNAi animals showed strong ectopic *sfrp-1* expression at the posterior pole as well as expanding expression along the midline and at the edge of the animal (Figure 6E). In contrast, irradiated β -catenin RNAi animals suffered from head regression, a phenotype previously observed for stem cell-depleted planarians (Reddien and Sánchez Alvarado, 2004), but did not induce *sfrp-1* in their tails. Similarly, ectopic *sfrp-1* induction was abolished by irradiation in regenerating *tsh* RNAi planarians (Figure S6C). These data sug-

gest that stem cells are required for the manifestation of the β -catenin RNAi phenotype.

Taken together, our data support a model in which, rather than undergoing a fate switch of existing muscle cells, β -catenin RNAi animals induce anterior determinants in newborn cells.

DISCUSSION

β -Catenin-Responsive Genes and Cell Types along the AP Axis

To shed light onto β -catenin-mediated control of tissue polarity, we identified hundreds of β -catenin-dependent genes with an RNA-seq-based screening approach. The set of candidate genes revealed a number of gut-associated genes, many of which were expressed by presumptive goblet cells. A tight link between Wnt signaling and the digestive system exists in the mammalian intestine, where this pathway controls progenitor proliferation and cell-lineage specification (Pinto et al., 2003; van de Wetering et al., 2002). However, because pathway induction did not elevate the expression of gut genes, and Wnt/ β -catenin RNAi planarians undergo severe remodeling events due to the regression of posterior tissues, we cannot exclude that the loss of gut-associated genes in these animals might be an indirect effect.

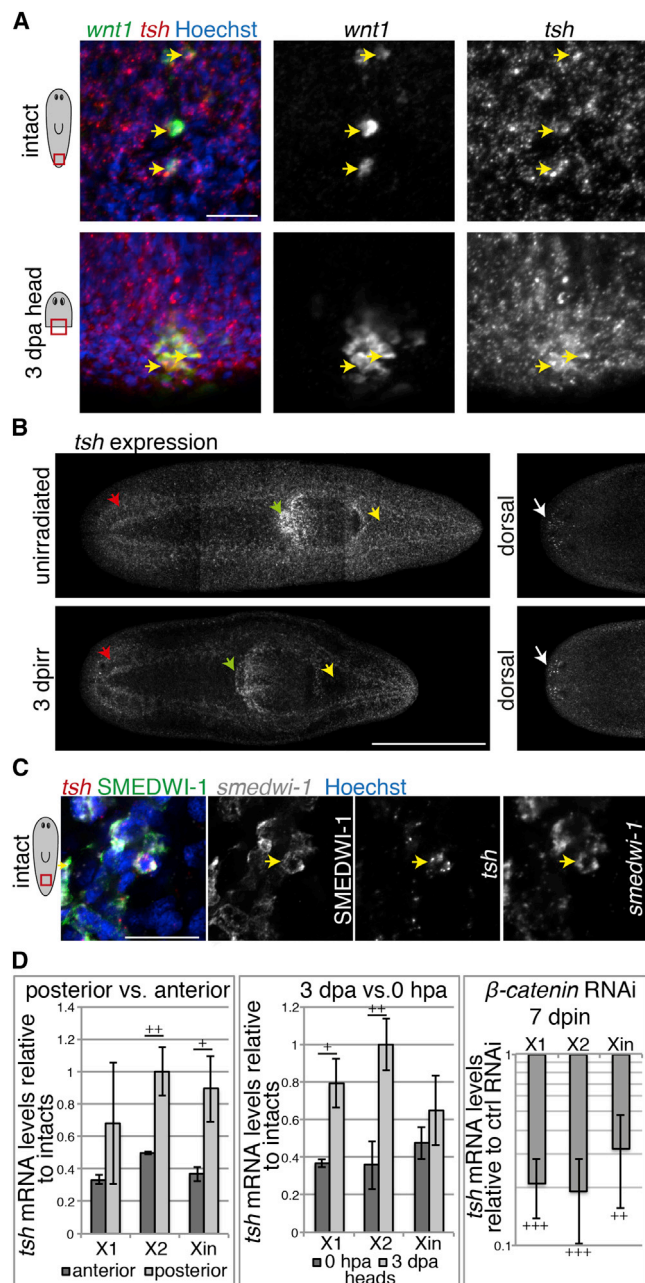


Figure 5. *tsh* Is Expressed in *wnt1*-Positive Cells and Marks a Subpopulation of Stem Cells

(A) Double FISH of *tsh* (red) and *wnt1* (green) on intact animals (upper panels) and head fragments at 3 days postamputation (dpa) (lower panels). Yellow arrows indicate coexpression.

(B) *tsh* expression 3 days postirradiation (dpirr) and in unirradiated planarians. Parenchymal *tsh* levels (yellow arrow) are reduced whereas expression in the nervous system (red arrow), the pharynx (green arrow), and distinct dorsal cells in the head (white arrow) remains.

(C) Double FISH against *tsh* and *smedwi-1* combined with an immunostaining against SMEDWI-1. Yellow arrow indicates a triple-positive cell in the posterior of intact planarians.

(D) qPCR analysis of *tsh* expression on cell fraction X1 (4C), X2 (2C) and Xin (2C; irradiation insensitive) isolated by FACS by size and DNA content. Left panel, *tsh* expression in postpharyngeal (posterior) and prepharyngeal

Many of the β -catenin-dependent genes were differentially expressed along the AP axis, with high levels in the posterior. Several of them were induced in subepidermal muscle cells, which are known to express different sets of PCGs according to their location along the planarian body axes. Because they produce the putative Wnt receptor *fz-4* (Witchley et al., 2013), muscle cells might be indeed competent for Wnt signal transduction and interpret a β -catenin activity gradient along the AP axis.

At least three transcription factor genes identified in our data set (*sp5*, *abdBa*, *tsh*) were elevated in stem cell-enriched FACS fractions in a β -catenin-dependent manner. Additionally, transcripts associated to a stem cell lineage, giving rise to epidermal cells (van Wolfswinkel et al., 2014), were strongly downregulated after β -catenin RNAi. This indicates that, in addition to muscle cells, stem cells adjust their expression profile to changes in β -catenin signaling. The previously proposed heterogeneity of the planarian stem cell pool (Reddien, 2013; Scimone et al., 2014; van Wolfswinkel et al., 2014) may therefore be, at least in part, due to signaling gradients along the planarian body axes. Whether this response is a direct one or is induced through nonautonomous signals provided by muscle cells remains an open question.

Several Wnt pathway components were differentially expressed upon β -catenin depletion, and similar genes were also found in zebrafish fin regeneration data sets (Wehner et al., 2014) (Table 1). As canonical Wnt signaling is thought to form robust feedback loops during development by regulating its own components and inhibitors (Wawra et al., 2007), our data support the hypothesis that these feedback loops are conserved in regenerative processes. Interestingly, RNAi against β -catenin induced *ndk*, an FGF receptor-like gene with a nonfunctional kinase domain that is suggested to restrict the spreading of an unknown brain-inducing FGF ligand to the head (Cebrià et al., 2002). Given that we identified a number of FGF-related genes in our data set (Data S1), it is possible that antagonizing FGF and WNT activities are required to ensure correct tissue identity and patterning along an AP axis.

tsh as a Regulator of AP Polarity

tsh is expressed in *wnt1* gene-expressing cells, presumably subepidermal muscle cells, and in a subpopulation of stem cells, in a β -catenin-dependent manner. RNAi experiments in planarians revealed *tsh* as a suppressor of anterior tissues during regeneration and homeostasis. Because *tsh* RNAi phenocopies depletion of essential Wnt/ β -catenin signaling components, and *tsh*

(anterior) cell fractions. Expression levels were normalized to intact, and percentage of peak expression is shown. Middle panel, *tsh* expression in cell fractions of head fragments at 0 hr postamputation (hpa) and 3 dpa. Expression levels were normalized to intact, and percentage of peak expression is shown. Right panel, *tsh* expression in cell fractions after β -catenin RNAi 7 days after last injection. Expression in cell fractions from homeostatic β -catenin RNAi animals was normalized to the corresponding control RNAi cell fractions. Error bars, SD of three biological replicates. Significance (Student's *t* test) is indicated (+, $p \leq 0.05$; ++, $p \leq 0.01$; +++, $p \leq 0.001$).

Scale bars, 500 μ m in (B), 20 μ m in (A) and (C). DNA is blue (Hoechst). See also Figure S5.

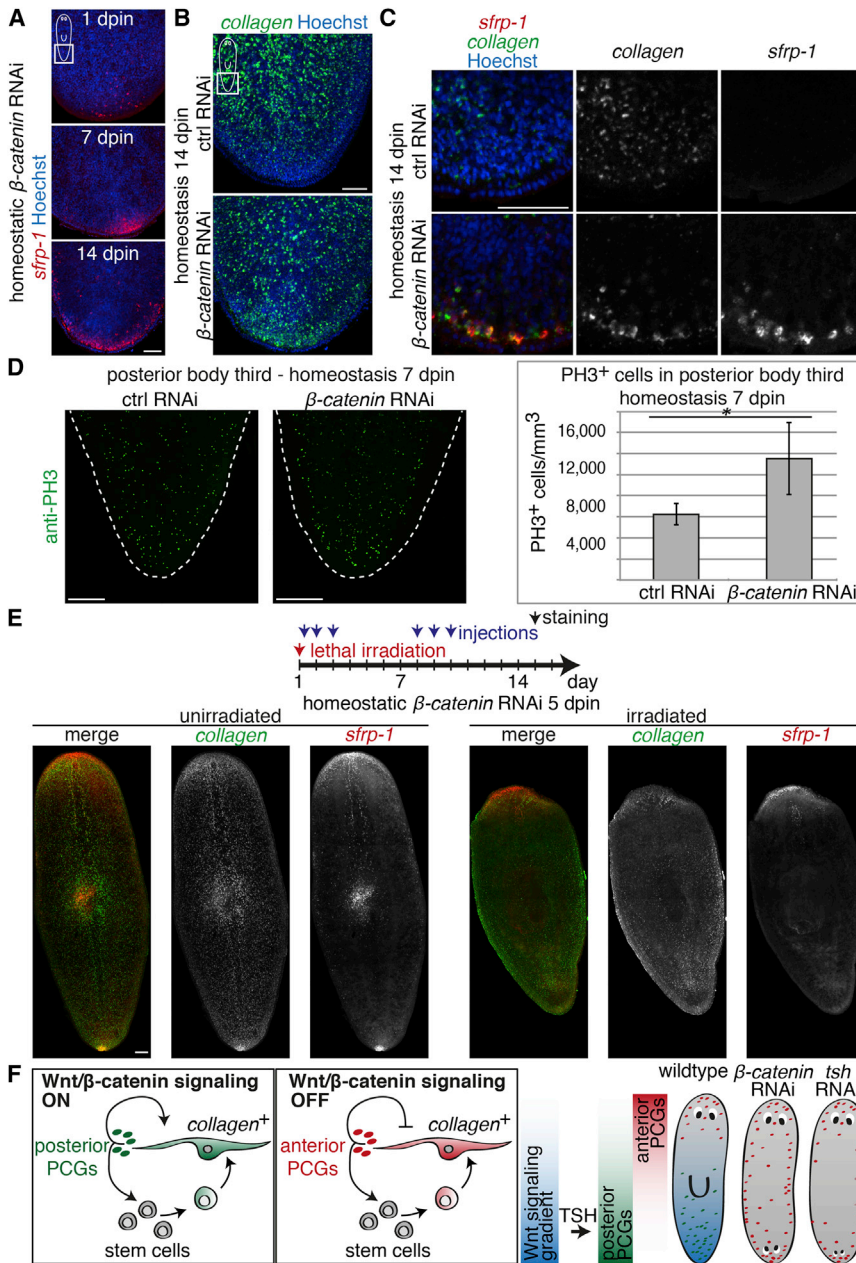


Figure 6. Ectopic Expression of Anterior Genes after β -catenin RNAi Is Stem Cell Dependent and Accompanied by Enhanced Muscle Formation

(A) Fluorescent in situ hybridization (FISH) for the anterior marker gene *sfrp-1* (red) at 1, 7, and 14 days after dsRNA injection (dpn). *sfrp*-expressing cells accumulate in the tail of homeostatic β -catenin RNAi animals over time.

(B) FISH of the muscle marker *collagen* (green) on homeostatic β -catenin RNAi animals compared to control (ctrl) RNAi animals at 14 dpn. *collagen*-expressing cells accumulate in homeostatic β -catenin RNAi.

(C) Double FISH of *sfrp-1* (red) and *collagen* (green) on homeostatic animals at 14 dpn.

(D) Immunostaining of phosphorylated HISTONE 3 (PH3) on homeostatic ctrl and β -catenin RNAi animals at 7 dpn. Positive cells within posterior third of the body were counted. β -catenin RNAi causes a significant increase in the number of mitotic cells. $p < 0.05$; $n = 4$.

(E) *collagen* and *sfrp-1*-expressing cells accumulate in β -catenin RNAi animals but not after depletion of stem cells by γ -irradiation. γ -irradiation was followed by 2 weeks of dsRNA injection and FISH analysis 5 dpn.

(F) Model of β -catenin-dependent AP control. In planarians, new muscle cells form during regeneration and tissue turnover. In the head, where Wnt/ β -catenin activity is low, muscle cells express anterior position control genes (PCGs). In the tail, where signaling is high, muscle cells induce posterior PCGs. Posterior PCGs may promote Wnt/ β -catenin signaling, whereas anterior PCGs may act as inhibitors. Upon β -catenin inhibition, muscle cells of anterior identity form in the tail, causing a posterior-to-anterior transformation and two-headed planarians. TSH might be a downstream mediator of Wnt/ β -catenin signaling required for appropriate PCG expression.

Scale bars, 100 μ m in (D) and (E), 50 μ m in (A)–(C). DNA (Hoechst) is blue. See also Figure S6.

levels are reduced in the posterior after *wnt1* and β -catenin RNAi, TSH might be a transducer of canonical Wnt signaling downstream of or in synergy with β -CATENIN activity. This model is consistent with studies in *Drosophila* and *Xenopus*, where Tsh modulates β -catenin activity, possibly through a direct interaction (Gallet et al., 1998; Onai et al., 2007). In *Drosophila*, *tsh* acts as a homeotic gene and is involved in several Hox-dependent body patterning processes such as specifying the embryonic trunk (Fasano et al., 1991; de Zulueta et al., 1994; Röder et al., 1992). As homeobox genes were found in the Wnt/ β -catenin-dependent data sets from planarians and zebrafish, a link between *tsh* and this transcription factor family may be conserved.

differences in protein turnover and hence differential depletion of TSH and β -CATENIN proteins after RNAi and/or an engagement of *tsh* only in a subset of β -catenin-dependent processes. We also detected a phenotypic difference between *tsh* and β -catenin RNAi animals already at 18 hpa, during the presumptive polarity phase. Although anterior *notum* expression was abolished after β -catenin RNAi (Petersen and Reddien, 2011), early *notum* expression was not changed at anterior wounds of *tsh* RNAi planarians. Expression analysis revealed that *tsh* is induced, similar to *wnt1*, earlier than other posterior *wnt* genes during regeneration (Gurley et al., 2010). In addition, the inhibition of *wnt11-1*, *-2*, and *-5* expression after *tsh* RNAi suggests that *tsh*, like *wnt1*, acts upstream of these genes during tail

regeneration, possibly in a feedback loop. This is consistent with the absence of a two-headed phenotype after *wnt11-1*, *-2*, and *-5* RNAi (Adell et al., 2009; Gurley et al., 2008), in contrast to *wnt1* and *tsh* RNAi regenerates.

What might be the cellular basis for homeotic tissue transformation after β -catenin depletion? We identified an accumulation of cells expressing anterior PCGs and markers for the muscle lineage at posterior and lateral sites, accompanied by increased cell proliferation. This accumulation was dependent on the presence of stem cells, suggesting that phenotypic manifestation may require the differentiation of stem cells into muscle cells. Which signals induce such massive differentiation is not clear, yet its local occurrence points to the presence or absence of signals from specific locations. We conclude that differential Wnt/ β -catenin signaling levels along the AP axis may control the identity of differentiating cells during regeneration and constant tissue turnover (model in Figure 6).

EXPERIMENTAL PROCEDURES

Planarians

All experiments were performed with a clonal line of asexual planarians of the species *Schmidtea mediterranea* (provided by E. Saló) maintained at 20°C in Montjuïc salts solution (Cebrià and Newmark, 2005). Animals were fed with veal liver and starved for at least 7 days prior to experiments.

Exposure to Irradiation

For lethal irradiation, planarians were exposed to 6,000 rad using a Gamma-cell-40 Exactor (Nordion) with two Caesium-137 sources delivering ~92 rads/min. RNAi animals were cut 1 day after lethal irradiation for regeneration experiments.

RNAi

RNAi was performed as previously described (Sandmann et al., 2011). In the case of double-knockdown experiments, 1.5 μ g/ μ l of each dsRNA (3 μ g/ μ l total) was injected. dsRNA against *green fluorescent protein (gfp)* was injected in control animals. Animals were amputated pre-/postpharyngeally to observe regeneration for the time indicated, or animals were left uncut for the indicated times to observe homeostatic phenotypes. Live images were taken with a Leica M80 microscope. Primer sequences for dsRNA generation are listed in Data S4.

In Situ Hybridization

Whole-mount in situ hybridization (WISH) was performed as previously described (Nogi and Levin, 2005; Umesono et al., 1999) using the In situPro VSi hybridization robot (Intavis). WISH images were taken with a Leica M165 FC microscope. Fluorescent whole-mount in situ hybridization (FISH) was performed as previously described (Cebrià and Newmark, 2005; März et al., 2013). Nuclear staining was performed with Hoechst 33342 (Life Technologies). FISH images were taken with a Zeiss LSM700 or LSM780 confocal laser-scanning microscope and processed with Fiji and Adobe Photoshop CS5. Signal intensities along AP were measured with Fiji. Primers sequences for probe generation and references for marker genes are listed in Data S4.

Immunohistochemistry

Immunostainings were performed as previously described (Cebrià and Newmark, 2005). Antibodies were rabbit anti-SMEDWI-1 (1:1,000) (Guo et al., 2006; März et al., 2013), mouse anti-SYNORF (3C11; 1:50; Developmental Studies Hybridoma Bank), mouse anti-Arrestin (VC-1; 1:15,000; H. Orii), and rabbit anti-phospho-Histone H3 (PH3) (1:600; Millipore). Rabbit anti-RPZ-1 was generated with BioGenes (peptide C-IDTDTKKNYNEQYQ) and used in a 1:200 dilution. Secondary antibodies were Alexa 488 goat anti-mouse and Alexa 647 goat anti-rabbit (Molecular Probes).

Quantitative PCR

RNA extraction, cDNA synthesis, and quantitative PCR (qPCR) was performed as previously described (Sandmann et al., 2011), and relative quantification of gene expression was calculated according to Pfaffl (2001). *gapdh* served as an internal reference gene. Primers are listed in Data S4.

Fluorescence-Activated Cell Sorting

Planarian cell dissociation was performed as described in Moritz et al. (2012). Fluorescence-activated cell sorting (FACS) by DNA content (Hoechst blue) and cell size (Hoechst red) was performed with the FACSAria Cell Sorter (BD Biosciences) and its respective software. Three biological replicates were individually sorted for each sample.

Sample Collection and Preparation for β -catenin and notum RNAi RNA-Seq

Planarians were injected with dsRNAs against *\beta*-catenin or *gfp* on 3 consecutive days for 2 weeks (total six times) and left uncut for 7 days. Tails were cut off and processed for RNA extraction. Two biological replicates of 30 fragments each were prepared. To generate *notum* RNAi libraries, total RNA was extracted from *gfp* and *notum* RNAi tail stumps at 0 and 18 hr postamputation (two rounds of regeneration). Sequencing libraries were prepared from 1 μ g RNA according to the TruSeq RNA Sample Prep v2 LS protocol.

Illumina Single-End Sequencing and Differential Expression

Analysis

Libraries were sequenced on an Illumina HiScanSQ. See the Supplemental Experimental Procedures for details on data processing and analysis.

Transcriptome Comparisons

Comparisons of the transcriptomes after *\beta*-catenin and *notum* RNAi were generated using a custom R script. See text and the Supplemental Experimental Procedures for details.

Zebrafish Experiments

Experiments with adult zebrafish have been approved by the state of Baden-Württemberg and the animal protection representative of Ulm University. Partial resection of the caudal fins and processing of regenerates for whole-mount in situ hybridization was performed as described previously (Poss et al., 2000a, 2000b). Transgenic fish lines used were *hsp70l:dkk1-GFP^{w32}* (*hs:dkk1* [Stoick-Cooper et al., 2007] and *hsp70l:Mmu.Axin1-YFP^{w35}* [*hs:Axin1*; Kagermeier-Schenk et al., 2011]). Heat shocks were performed for 1 hr at 37°C as described (Wehner et al., 2014).

ACCESSION NUMBERS

Data have been deposited to GenBank and are available under accession numbers KP003814 (*Smed-rapunzel-1*), KP003815 (*Smed-teashirt*), KP003816 (*tr5_12233*), KP003817 (*Smed-ptk7*), and KP003818 (*Smed-sp5*). Sequencing data are deposited as Bioproject PRJNA252403/SRR043140:SRX591269/SRR1380987 (GFP 18 hr), SRX591272/SRR1380989 (*notum* 18 hr), SRX595663/SRR1390644(GFP/tail), and SRX591270/SRR1380986 (*bcat/tail*). Transcriptome assembly and reads have been deposited as Bioproject PRJNA252663/SRR043189.

SUPPLEMENTAL INFORMATION

Supplemental Information includes Supplemental Experimental Procedures, six figures, two tables, and four data sets and can be found with this article online at <http://dx.doi.org/10.1016/j.celrep.2014.12.018>.

AUTHOR CONTRIBUTIONS

H.R. and K.B. conceived the study; H.R., M.M., M.C.V., S.O., T.A., and K.B. designed experiments; H.R., M.M., M.C.V., L.G.-B., and S.O. performed all planarian experiments; H.R., M.M., M.C.V., S.O., T.A., and K.B. analyzed and interpreted the data. D.W. and G.W. contributed zebrafish data and the

corresponding figure; D.E. assembled the reference transcriptome, performed RNA-seq data analysis, and contributed the phylogenetic tree. All authors contributed to writing and editing the manuscript.

ACKNOWLEDGMENTS

We thank M. Sinn for Illumina library preparation and sequencing; F. Konert and S. Pavelka for excellent technical assistance; Y. Perez Rico for bioinformatics assistance; DSHB for the anti-SYNORF1 antibody; H. Orii for the anti-Arrestin antibody (VC-1); F. Cebrià, E. Saló, M. Almuedo-Castillo, and members of the K.B. and Gentile labs for helpful discussions. This work was funded by the Max Planck Society and the Deutsche Forschungsgemeinschaft (SFB629). H.R. was funded by a stipend from the CiM-IMPRS graduate school. L.G.-B. was supported by the ERASMUS program. Research in the G.W. lab is supported by grant WE 4223/4-1 of the Deutsche Forschungsgemeinschaft. The K.B. lab is part of the Cells-in-Motion Cluster of Excellence (EXC 1003-CiM).

Received: June 13, 2014

Revised: November 7, 2014

Accepted: December 9, 2014

Published: December 31, 2014

REFERENCES

- Adell, T., Saló, E., Boutros, M., and Bartscherer, K. (2009). Smed-Evi/Wntless is required for beta-catenin-dependent and -independent processes during planarian regeneration. *Development* 136, 905–910.
- Adell, T., Cebrià, F., and Saló, E. (2010). Gradients in planarian regeneration and homeostasis. *Cold Spring Harb. Perspect. Biol.* 2, a000505.
- Buckingham, M., and Rigby, P.W. (2014). Gene regulatory networks and transcriptional mechanisms that control myogenesis. *Dev. Cell* 28, 225–238.
- Cebrià, F., and Newmark, P.A. (2005). Planarian homologs of netrin and netrin receptor are required for proper regeneration of the central nervous system and the maintenance of nervous system architecture. *Development* 132, 3691–3703.
- Cebrià, F., Kobayashi, C., Umesono, Y., Nakazawa, M., Mineta, K., Ikeo, K., Gojobori, T., Itoh, M., Taira, M., Sánchez Alvarado, A., and Agata, K. (2002). FGFR-related gene *nou-darake* restricts brain tissues to the head region of planarians. *Nature* 419, 620–624.
- Chai, G., Ma, C., Bao, K., Zheng, L., Wang, X., Sun, Z., Saló, E., Adell, T., and Wu, W. (2010). Complete functional segregation of planarian beta-catenin-1 and -2 in mediating Wnt signaling and cell adhesion. *J. Biol. Chem.* 285, 24120–24130.
- Clevers, H. (2006). Wnt/beta-catenin signaling in development and disease. *Cell* 127, 469–480.
- de Zulueta, P., Alexandre, E., Jacq, B., and Kerridge, S. (1994). Homeotic complex and *teashirt* genes co-operate to establish trunk segmental identities in *Drosophila*. *Development* 120, 2287–2296.
- Eisenhoffer, G.T., Kang, H., and Sánchez Alvarado, A. (2008). Molecular analysis of stem cells and their descendants during cell turnover and regeneration in the planarian *Schmidtea mediterranea*. *Cell Stem Cell* 3, 327–339.
- Fasano, L., Röder, L., Coré, N., Alexandre, E., Vola, C., Jacq, B., and Kerridge, S. (1991). The gene *teashirt* is required for the development of *Drosophila* embryonic trunk segments and encodes a protein with widely spaced zinc finger motifs. *Cell* 64, 63–79.
- Felix, D.A., and Aboobaker, A.A. (2010). The TALE class homeobox gene *Smed-prep* defines the anterior compartment for head regeneration. *PLoS Genet.* 6, e1000915.
- Gallet, A., Erkner, A., Charroux, B., Fasano, L., and Kerridge, S. (1998). Trunk-specific modulation of wingless signalling in *Drosophila* by *teashirt* binding to *armadillo*. *Curr. Biol.* 8, 893–902.
- Guo, T., Peters, A.H., and Newmark, P.A. (2006). A Bruno-like gene is required for stem cell maintenance in planarians. *Dev. Cell* 11, 159–169.
- Gurley, K.A., Rink, J.C., and Sánchez Alvarado, A. (2008). Beta-catenin defines head versus tail identity during planarian regeneration and homeostasis. *Science* 319, 323–327.
- Gurley, K.A., Elliott, S.A., Simakov, O., Schmidt, H.A., Holstein, T.W., and Sánchez Alvarado, A. (2010). Expression of secreted Wnt pathway components reveals unexpected complexity of the planarian amputation response. *Dev. Biol.* 347, 24–39.
- Hayashi, T., Asami, M., Higuchi, S., Shibata, N., and Agata, K. (2006). Isolation of planarian X-ray-sensitive stem cells by fluorescence-activated cell sorting. *Dev. Growth Differ.* 48, 371–380.
- Iglesias, M., Gomez-Skarmeta, J.L., Saló, E., and Adell, T. (2008). Silencing of *Smed-betacatenin1* generates radial-like hypercephalized planarians. *Development* 135, 1215–1221.
- Iglesias, M., Almuedo-Castillo, M., Aboobaker, A.A., and Saló, E. (2011). Early planarian brain regeneration is independent of blastema polarity mediated by the Wnt/beta-catenin pathway. *Dev. Biol.* 358, 68–78.
- Kagermeier-Schenk, B., Wehner, D., Ozhan-Kizil, G., Yamamoto, H., Li, J., Kirchner, K., Hoffmann, C., Stern, P., Kikuchi, A., Schambony, A., and Weidinger, G. (2011). *Waif1/5T4* inhibits Wnt/beta-catenin signaling and activates noncanonical Wnt pathways by modifying LRP6 subcellular localization. *Dev. Cell* 21, 1129–1143.
- Kao, D., Felix, D., and Aboobaker, A. (2013). The planarian regeneration transcriptome reveals a shared but temporally shifted regulatory program between opposing head and tail scenarios. *BMC Genomics* 14, 797.
- Kawakami, Y., Rodriguez Esteban, C., Raya, M., Kawakami, H., Martí, M., Dubova, I., and Izpisua Belmonte, J.C. (2006). Wnt/beta-catenin signaling regulates vertebrate limb regeneration. *Genes Dev.* 20, 3232–3237.
- Koebnick, K., Kashef, J., Pieler, T., and Wedlich, D. (2006). *Xenopus* *Teashirt1* regulates posterior identity in brain and cranial neural crest. *Dev. Biol.* 298, 312–326.
- Liu, S.Y., Selck, C., Friedrich, B., Lutz, R., Vila-Farré, M., Dahl, A., Brandl, H., Lakshmanaperumal, N., Henry, I., and Rink, J.C. (2013). Reactivating head regrowth in a regeneration-deficient planarian species. *Nature* 500, 81–84.
- März, M., Seebeck, F., and Bartscherer, K. (2013). A *Pitx* transcription factor controls the establishment and maintenance of the serotonergic lineage in planarians. *Development* 140, 4499–4509.
- Moritz, S., Stöckle, F., Ortmeier, C., Schmitz, H., Rodríguez-Esteban, G., Key, G., and Gentile, L. (2012). Heterogeneity of planarian stem cells in the S/G2/M phase. *Int. J. Dev. Biol.* 56, 117–125.
- Nogi, T., and Levin, M. (2005). Characterization of *innexin* gene expression and functional roles of gap-junctional communication in planarian regeneration. *Dev. Biol.* 287, 314–335.
- Nogi, T., and Watanabe, K. (2001). Position-specific and non-colinear expression of the planarian posterior (*Abdominal-B-like*) gene. *Dev. Growth Differ.* 43, 177–184.
- Onai, T., Matsuo-Takasaki, M., Inomata, H., Aramaki, T., Matsumura, M., Yakura, R., Sasai, N., and Sasai, Y. (2007). *XTsh3* is an essential enhancing factor of canonical Wnt signaling in *Xenopus* axial determination. *EMBO J.* 26, 2350–2360.
- Orii, H., Kato, K., Umesono, Y., Sakurai, T., Agata, K., and Watanabe, K. (1999). The planarian *HOM/HOX* homeobox genes (*Plox*) expressed along the antero-posterior axis. *Dev. Biol.* 210, 456–468.
- Pellettieri, J., Fitzgerald, P., Watanabe, S., Mancuso, J., Green, D.R., and Sánchez Alvarado, A. (2010). Cell death and tissue remodeling in planarian regeneration. *Dev. Biol.* 338, 76–85.
- Petersen, C.P., and Reddien, P.W. (2008). *Smed-betacatenin-1* is required for anteroposterior blastema polarity in planarian regeneration. *Science* 319, 327–330.
- Petersen, C.P., and Reddien, P.W. (2009). A wound-induced Wnt expression program controls planarian regeneration polarity. *Proc. Natl. Acad. Sci. USA* 106, 17061–17066.

- Petersen, C.P., and Reddien, P.W. (2011). Polarized notum activation at wounds inhibits Wnt function to promote planarian head regeneration. *Science* 332, 852–855.
- Pfaffl, M.W. (2001). A new mathematical model for relative quantification in real-time RT-PCR. *Nucleic Acids Res.* 29, e45.
- Pinto, D., Gregorieff, A., Begthel, H., and Clevers, H. (2003). Canonical Wnt signals are essential for homeostasis of the intestinal epithelium. *Genes Dev.* 17, 1709–1713.
- Poss, K.D., Shen, J., and Keating, M.T. (2000a). Induction of *lef1* during zebrafish fin regeneration. *Dev. Dyn.* 219, 282–286.
- Poss, K.D., Shen, J., Nechiporuk, A., McMahon, G., Thisse, B., Thisse, C., and Keating, M.T. (2000b). Roles for Fgf signaling during zebrafish fin regeneration. *Dev. Biol.* 222, 347–358.
- Reddien, P.W. (2013). Specialized progenitors and regeneration. *Development* 140, 951–957.
- Reddien, P.W., and Sánchez Alvarado, A. (2004). Fundamentals of planarian regeneration. *Annu. Rev. Cell Dev. Biol.* 20, 725–757.
- Röder, L., Vola, C., and Kerridge, S. (1992). The role of the *teashirt* gene in trunk segmental identity in *Drosophila*. *Development* 115, 1017–1033.
- Sandmann, T., Vogg, M.C., Owlarn, S., Boutros, M., and Bartscherer, K. (2011). The head-regeneration transcriptome of the planarian *Schmidtea mediterranea*. *Genome Biol.* 12, R76.
- Scimone, M.L., Kravarik, K.M., Lapan, S.W., and Reddien, P.W. (2014). Neoblast specialization in regeneration of the planarian *Schmidtea mediterranea*. *Stem Cell Rev.* 3, 339–352.
- Sikes, J.M., and Newmark, P.A. (2013). Restoration of anterior regeneration in a planarian with limited regenerative ability. *Nature* 500, 77–80.
- Stoick-Cooper, C.L., Weidinger, G., Riehle, K.J., Hubbert, C., Major, M.B., Fausto, N., and Moon, R.T. (2007). Distinct Wnt signaling pathways have opposing roles in appendage regeneration. *Development* 134, 479–489.
- Umesono, Y., Watanabe, K., and Agata, K. (1999). Distinct structural domains in the planarian brain defined by the expression of evolutionarily conserved homeobox genes. *Dev. Genes Evol.* 209, 31–39.
- Umesono, Y., Tasaki, J., Nishimura, Y., Hrouda, M., Kawaguchi, E., Yazawa, S., Nishimura, O., Hosoda, K., Inoue, T., and Agata, K. (2013). The molecular logic for planarian regeneration along the anterior–posterior axis. *Nature* 500, 73–76.
- van de Wetering, M., Sancho, E., Verweij, C., de Lau, W., Oving, I., Hurlstone, A., van der Horn, K., Battle, E., Coudreuse, D., Haramis, A.P., et al. (2002). The beta-catenin/TCF-4 complex imposes a crypt progenitor phenotype on colorectal cancer cells. *Cell* 111, 241–250.
- van Wolfswinkel, J.C., Wagner, D.E., and Reddien, P.W. (2014). Single-cell analysis reveals functionally distinct classes within the planarian stem cell compartment. *Cell Stem Cell* 15, 326–339.
- Wagner, D.E., Wang, I.E., and Reddien, P.W. (2011). Clonogenic neoblasts are pluripotent adult stem cells that underlie planarian regeneration. *Science* 332, 811–816.
- Wawra, C., Kühl, M., and Kestler, H.A. (2007). Extended analyses of the Wnt/beta-catenin pathway: robustness and oscillatory behaviour. *FEBS Lett.* 581, 4043–4048.
- Wehner, D., Cizelsky, W., Vasudevaro, M.D., Ozhan, G., Haase, C., Kagermeier-Schenk, B., Röder, A., Dorsky, R.I., Moro, E., Argenton, F., et al. (2014). Wnt/ β -catenin signaling defines organizing centers that orchestrate growth and differentiation of the regenerating zebrafish caudal fin. *Cell Reports* 6, 467–481.
- Wenemoser, D., and Reddien, P.W. (2010). Planarian regeneration involves distinct stem cell responses to wounds and tissue absence. *Dev. Biol.* 344, 979–991.
- Witchley, J.N., Mayer, M., Wagner, D.E., Owen, J.H., and Reddien, P.W. (2013). Muscle cells provide instructions for planarian regeneration. *Cell Reports* 4, 633–641.
- Zayas, R.M., Cebrià, F., Guo, T., Feng, J., and Newmark, P.A. (2010). The use of lectins as markers for differentiated secretory cells in planarians. *Dev. Dyn.* 239, 2888–2897.